FLEXURAL BEHAVIOR OF FRP BARS AFTER EXPOSURE TO ELEVATED TEMPERATURES

Sherif E. El Gamal[1, 2] *, Abdulrahman M. Al-Fahdi[1], Mohammed Meddah[1], Abdullah Al-Saidy[1], and Kazi Md Abu Sohel[1]

[1]Civil and Architectural Engineering, Sultan Qaboos University, Muscat, Oman

[2]Menoufia University, Shebin El-Kom, Egypt

ABSTRACT: This study investigates the flexural behavior of fibre-reinforced polymer (FRP) bars after being subjected to different levels of elevated temperatures (100, 200 and 300°C). Three types of glass FRP bars (ribbed, sand coated, and helically wrapped) and one type of carbon FRP bars (sand coated) were used in this study. Two testing scenarios were used: (a) testing specimens immediately after heating and (b) keeping specimens to cool down to room temperature before testing. Test results showed that as the temperature increased the flexural strength and modulus of the tested FRP bars decreased. At temperatures higher than the glass transition temperature (T_g), significant flexural strength and modulus losses were recorded. Smaller diameter bars showed better residual flexural strength and modulus than the larger diameter bars. The immediately tested bars showed significant strength and modulus losses compared to bars tested after cooling. Different types of GFRP bars showed comparable results. However, the helically wrapped bars showed the highest flexural strength losses (37 and 60%) while the sand coated bars showed the lowest losses (29 and 39%) after exposure to 200 and 300°C, respectively. The carbon FRP bars showed residual flexural strengths comparable to those recorded for the GFRP bars; however, they showed lower residual flexural modulus after being subjected to 200 and 300°C.

Keywords: Fibre-reinforced polymer bars; FRP; Glass FRP; Carbon FRP; Flexural strength; Flexural modulus; Elevated temperatures; Bar diameters.

سلوك الإنثناء لقضبان البوليمر المقوى بالألياف بعد تعرضها لدرجات حرارة مرتفعة

شريف الجمل*, عبدالرحمن الفهدي, محمد مداح, عبدالله السعيدي, و كازي ابو سهيل

الملخص: تبحث هذه الدراسة في سلوك الانثناء لقضبان البوليمر المقوى بالألياف بعد تعرضها لمستويات مختلفة من درجات الحرارة المرتفعة (100 ، 200 ، 300 درجة مئوية). استخدمت في هذه الدراسة ثلاثة أنواع من قضبان البوليمر المقوى بالألياف الزجاجية (مضلع ، مغلف بالرمل ، وملفوف حلزونيًا) ونوع واحد من قضبان البوليمر المقوى بالألياف الكربونية (مغلفة بالرمل). تم استخدام سيناريوهين للإختبار: أ) اختبار العينات مباشرة بعد التسخين و ب) الاحتفاظ بالعينات لتبرد إلى درجة حرارة الغرفة قبل الإختبار. أظهرت نتائج الإختبار أنه كلما زادت درجة الحرارة انخفضت قوة و جساءة القضبان ضد الانثناء. عند درجات حرارة أعلى من درجة حرارة التزجج (T_g) ، تم تسجيل هبوط كبير في القوة والجساءة ضد الانثناء. أظهرت القضبان ذات الأقطار الصغيرة قوة و جساءة إنثناء أفضل من القضبان ذات الأقطار الكبيرة. أظهرت القضبان التي تم اختبارها على الفور نقص كبير في القوة والجساءة مقارنة بالقضبان التي تم اختبارها بعد انخفاض حرارتها. أظهرت الأنواع المختلفة من قضبان البوليمر المقوى بالألياف الزجاجية نتائج متقاربة. ومع ذلك ، أظهرت القضبان الملفوفة حلزونيًا أعلى خسائر في مقاومة الانثناء (37 و 60٪) بينما أظهرت القضبان المغطاة بالرمل أقل خسائر (29 و 39٪) بعد التعرض إلى 200 و 300درجة مئوية على التوالي. أظهرت قضبان البوليمر المقوى بالألياف الكربونية قوة انثناء مماثلة لتلك المسجلة لقضبان البوليمر المقوى بالألياف الزجاجية ؛ ومع ذلك ، فقد أظهرت معامل جساءة منخفض بعد تعرضها لـ 200 و 300 درجة مئوية.

الكلمات المفتاحية: قضبان البوليمر المقوى بالألياف؛ الألياف الزجاجية؛ الألياف الكربونية؛ قوة الإنثناء ؛ درجات الحرارة المرتفعة؛ أقطار القضبان.

*Corresponding author's e-mail: sherif@squ.edu.om

DOI: 10.53540/tjer.vol18iss1pp12-19

1. INTRODUCTION

In recent years, Fiber Reinforced Polymers (FRP) have become one of the promising reinforcing materials in concrete structures. FRP reinforcing bars can be used instead of steel bars in reinforced concrete (RC) structures because of their excellent properties, which include corrosion resistance, high strength-to-weight ratio, appropriate fatigue performance, electric insulation and easy cutting and handling (El-Gamal *et al*. 2014). These advantages increased their use to repair existing structures (Al-Saidy et al. 2015, 2017; El-Gamal et al. 2019). They also increased their use instead of steel bars in several new reinforced concrete (RC) structures in corrosive environments such as bridge deck slabs, parking garage slabs, RC pavements, and RC columns (Benmokrane et al. 2007, 2008; El-Gamal et al. 2009; Thébeau et al. 2010; El-Gamal et al. 2010; Bouguerra et al, 2011; Dulude et al. 2011; El-Gamal and Alshareedah 2020 a, b). On the other hand, they have some disadvantages compared to steel including no ductility, lower elastic modulus and shear strength. In addition, they are very sensitive to elevated temperatures (Ashrafi et al. 2017; Bazli and Abolfazli 2020; Jafarzadeh and Nematzadeh 2020)

The wide use of FRP bars in concrete structures led to new challenges for engineers. One of these challenges is the performance of FRP bars when subjected to elevated temperatures. FRP bars performance is poor under elevated temperatures. As the temperature increases, the matrix softens at the glass transition temperature level (T_g). Above T_g, the matrix elastic modulus significantly reduces due to a change in its molecular structure. The thermal properties of fibres, however, are better than the matrix and can continue sustaining the load in a longitudinal direction until reaching the temperature level of the fibres. Engineers when designing a structure must consider the time that the structure can withstand high temperatures. Therefore, it is important to investigate the behavior of FRP bars subjected to elevated temperatures. Robert and Benmokrane (2010) investigated the tensile strength, shear strength and flexural strength of one type of glass FRP (GFRP) bar subjected to elevated temperatures. The elevated temperature levels ranged between 100 and 325°C. The results showed that the shear and the flexural strengths were much more sensitive to high temperature than the tensile strength. The flexural strength of the GFRP bars increased when the temperature decreased. At 120°C, the mechanical strength and flexural modulus dropped because of the change of the state of the polymer.

Alsayed *et al*. (2012) investigated the tensile properties of GFRP bars subjected to elevated temperatures for different periods. The study included two groups of specimens. The first group was 60 specimens without concrete cover (bare bars) with 1 m length. While the second group consisted of 60 specimens covered with concrete to represent the actual case when using the GFRP bars in concrete. The elevated temperatures used were 100, 200 and 300°C. The bars were tested in tension after exposure to the elevated temperatures. The authors concluded that the tensile strength decreased as the level of temperature or exposure period increased. The losses of tensile strength ranged between 3.1 to 35.1% and 9.7 to 41.9% for concrete-covered and bare GFRP bars, respectively.

Maranan *et al*. (2014) studied the flexural behavior of sand-coated GFRP bars of different diameters subjected to elevated temperatures up to 150°C. As the temperature increased, the flexural strength and modulus of the GFRP bars decreased. When approaches the T_g of the bars, the polymer changed from glassy (hard) material to rubbery (soft) material. The polymer begins to lose the ability to hold the fibre together and transfer stresses from one fibre to another. For all temperatures from 21 to 80°C, the load increased linearly with deflection up to failure. In addition, temperatures from 100 to 150°C exhibited a non-linear behavior and modulus degradation before reaching the maximum load because the T_g of the bar was about 117°C. The research recommended additional studies to provide further information that can be used to establish a relationship that can predict the tensile response of the GFRP bars from the bending response at elevated temperatures.

Ashrafi *et al*. (2017) investigated the physical and thermal properties of FRP bars subjected to elevated temperatures. The test specimens used were four types of FRP bars; sand-coated GFRP, helically wrapped CFRP, and grooved CFRP bars with two different resins (epoxy and vinyl ester). The research concluded that, as the temperature increased the tensile strength of the FRP bars decreased. Also, the bigger the diameter the greater tensile strength. The results of CFRP bars showed linear deformation until reaching the ultimate load. The critical temperatures of the sand-coated GFRP bars when losing 50% of its tensile strength were 300, 375, 377 and 450°C for 4, 6, 8, and 10 mm respectively. The critical temperatures of the three types of CFRP bars tested were 330, 360 and 450°C, respectively.

Hamad *et al*. (2017) studied the effect of elevated temperatures on the mechanical properties of FRP bars and the bond behavior between FRP bars and concrete. The test specimens used were four types; sand-coated CFRP, helically wrapped Basalt FRP (BFRP), helically wrapped GFRP, and Steel bars. The elevated temperatures used ranged between 125 to 450°C. After exposure to elevated temperatures, the specimens were left to cool in the air after taken from the electrical furnace. The tensile strength reduction of FRP bars was almost linear up to a critical temperature of 325°C. At a temperature of 450°C, the GFRP and BFRP bars melted and totally lost their tensile strength capacity. Steel bars had a minor reduction in tensile strength compared with the FRP bars. Among the FRP bars, the

CFRP showed the highest bond strength with concrete because of their better surface characteristics. However, steel bars attained the highest bond strength and modulus. The study recommended additional experimental work using other types of commercially available FRP bars.

The literature shows that few studies investigated the flexural behavior of the FRP bars subjected to elevated temperatures and recommended conducting more research on this topic. In addition, these studies are limited to specific types and diameters of the FRP bars. Therefore, to enrich the knowledge about this topic, it was decided to conduct this research study to investigate the flexural behavior of different types and diameters of FRP bars exposed to elevated temperatures. Test parameters include the four types of FRP bars (sand-coated GFRP, helically wrapped GFRP, grooved GFRP, and sand-coated CFRP), three diameters of the grooved GFRP bars (10, 16 and 20 mm), three target temperature levels (100, 200 and 300°C), and three exposure periods (1, 2 and 3 hours). In addition, two testing scenarios were investigated: a) testing specimens immediately after heating; and b) keeping specimens to cool down to room temperature before testing.

2. EXPERIMENTAL WORK

2.1. FRP Bars

Three different types of GFRP bars and one type of CFRP bars were used in this study. The GFRP bars included; a) grooved (G1) with nominal diameters of 10, 16 and 20 mm; b) sand-coated (G2) with a nominal diameter of 10 mm, and c) helically wrapped (G3) with a nominal diameter of 10 mm. While sand-coated CFRP (C1) bar with a nominal diameter of 10 mm was used. Table 1 presents the list of FRP types, manufacturers and their properties. Figure 1 shows photos of the bars used in this investigation.

2.2. Test Specimens and Parameters

FRP bars were prepared for flexure tests. The length of all specimens was 240 mm. The total number of specimens tested in this study was 99 specimens. Three specimens of each diameter were tested at room temperature as control specimens. The remaining specimens were exposed to temperatures of 100, 200, and 300°C for one hour. An electric furnace was used to heat up the specimens. The temperature was increased at a rate of 3°C degrees per minute until reaching the required temperature then was kept constant at the required temperature level. All the G1 specimens were tested using two testing scenarios. Half of them were tested immediately after taken out from the furnace. The other half was kept in the lab for one hour to cool down before testing. All other types of FRP bars were tested immediately after taken out from the furnace.

2.3. Flexural Test Procedure

All specimens were tested under a three-point bending test set-up. The flexural tests were conducted in accordance with the ASTM D790 standard (ASTM D790-03, 2003). The clear span between supports was 180 mm and the overhangs were 30 mm. The tests were carried out using a 600 kN MTS machine under a loading rate of 4 mm/min. The applied load and the mid-span deflection were recorded using a data logger. Figure 2 shows a typical specimen during the testing.

(a) Grooved GFRP Bars (G1).

(b) Sand-Coated GFRP Bar (G2).

(c) Helically wrapped GFRP Bar (G3).

(d) Sand-Coated CFRP Bar (C1).

Figure 1. FRP bars used in this study.

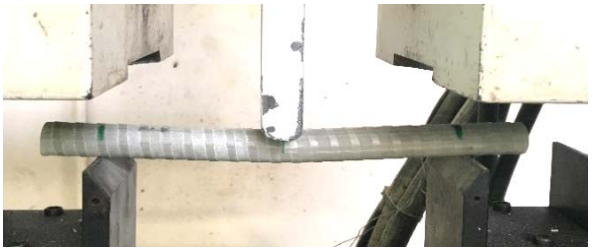

Figure 2. FRP specimen during flexure testing.

Table 1. Properties of FRP bars used in this study.

Type	Glass					Carbon
	G1[a]			G2[b]	G3[c]	C1[b]
Nominal Diameter	10	16	20	10	10	10
Tensile Strength (MPa)	1150	1102	1094	1185	849	1596
Tensile Modulus (GPa)	60.5	61.2	66.4	52.3	48.8	120
Ultimate strain (%)	1.9	1.8	1.65	2.26	1.81	1.33
Area (mm^2)	66.5	199	284	71.3	71.3	71.3

[a] Made in UAE; [b] made in Canada; [c] made in the USA.

3. TEST RESULTS AND DISCUSSIONS

3.1. Summary of Results

Table 2 summarizes the experimental test results of all tested bars. The values of the flexural strength and modulus presented are the average values from three specimens. The flexural strength (f_b) and the flexural modulus (E_b) were calculated using Eqn. (1) and Eqn. (2), respectively. More details about these equations can be found in Appendix A and Appendix B, respectively.

$$f_b = \frac{8FL}{\pi d_b^3} \quad (1)$$

$$E_b = \frac{(F_{50}-F_{20})}{(\Delta_{50}-\Delta_{20})}\frac{4L^3}{3\pi d_b^4} \quad (2)$$

where F, L, and d_b, are the maximum concentrated load, clear span, and nominal diameter of the bars, respectively; F_{50} *and* F_{20} are the concentrated load at 50 and 20% of the maximum load, respectively. Δ_{50} and Δ_{20} are the mid-span deflection at F_{50} *and* F_{20}, respectively.

The values of F *and* Δ in Eqn. (2) were obtained from the load-deflection curve of each bar. Specimens exposed to 100 and 200ºC showed a linear relationship between the load and mid-span deflection until failure for all FRP types. Some of the specimens exposed to 300ºC show nonlinear behavior at higher loads levels close to failure.

3.2. Failure Modes of Tested Bars

The general failure mode of most FRP bars after testing is defined by crushing of the bars in the compression zone and rupture of fibres in the tension side as shown in Fig. 3(a). Some of the 20 mm diameter bars showed an interlaminar shear failure at high temperatures (200 and 300°C) as shown in Fig. 3(b). It occurs due to high horizontal shear force that affected the weak matrix at high temperatures.

3.3 Effect of Temperature Level and Bar Diameter (Type G1 Bars)

Figures 4(a) and 4(b) represent the residual flexural strength of type G1 bars as a function of temperature level and bar diameter for both immediate and cooling testing scenarios, respectively. Figure 4(a) shows that, in the immediate scenario, the residual flexural strength decreased as the temperature level increased. After exposure for one hour to 100°C, the residual flexural strengths ranged between 78 to 84% of the control samples. The residual flexure strength was significantly affected after exposure to 200 and 300°C. At 200°C, the residual flexural strengths ranged between 19 and 67% and then reduced at 300°C to range between 11 and 48%. This decrease in the residual flexural strength at higher temperature levels could be related to the matrix softening. As the temperature exceeds the T_g temperature, the matrix elastic modulus significantly reduces due to a change in its molecular structure and results in lower efficiency in transferring shear forces between fibres, consequently, results in lower flexural strength of the FRP bars. Fig. 4(a) also shows that, in the immediate scenario, the flexural strength losses at 100°C was not affected by the bar diameter where the matrix at this temperature level was not significantly affected and the failure was dominant by the fibres. At this temperature level, the residual flexure strengths were 78, 84, and 84% for the 10, 16, and 20 mm diameter bars, respectively. At 200 and 300°C (higher than the Tg), it can be noticed that the residual strength decreased as the bar diameter increased. At 200°C, the residual flexural strengths were 67, 32, and 19% for the 10, 16, and 20 mm diameter bars, respectively. Similar observations were recorded at 300°C where the residual flexural strengths were 48, 31 and 11%, respectively. At these temperature levels, matrices become weak and the shear strength of the matrix dominants the failure. In smaller diameter bars, there are lower horizontal shear stresses in the matrix, which delays the matrix failure and results in higher residual strength. These shear stresses increase as the bar diameters increase and result in earlier failure of the matrix and lower flexural strength. This can be seen from the interlaminar shear failure observed in the 20 mm bars at high temperatures as shown in Fig. 3(b). This agrees with previous research studies (Robert and Benmokrane 2010; Maranan *et al*. 2014).

In the cooling scenario (Fig. 4(b)), it can be noticed that the residual flexural strength was not significantly affected by increasing the temperature level or bar diameter. The flexural strength losses ranged between 5 and 8%, 4 and 14%, and 3 and 12% for bars exposed to 100, 200 and 300°C temperatures, respectively. This indicates that allowing the temperature of the specimens to cool down before testing enhanced their strength and resulted in residual flexural strengths close to those of the reference specimens. This shows that the matrix gained strength after cooling and were able to transfer the shear forces between the fibres, which resulted in the high flexural strength values compared to the immediate scenario.

Figures 5(a) and 5(b) show the residual flexural modulus of all G1 bars for both immediate and cooling specimens, respectively. The modulus results were consistent with the strongest results. It can be noticed that, for the immediate scenario, the modulus decreased as the temperature level increased. The residual flexural modulus was only about 18% at 200 and 300°C for the 16 and 20 mm bars (losses of about 82%). This again could be related to the weakness of the resin due to high temperatures especially for bigger bars that did not lose heat during immediate testing. For cooling specimens, the used temperature levels have a slight effect on the flexural modulus of the tested bars. For example, the residual flexural moduli of the 10, 16 and 20 mm was 99, 98 and 92% at 200°C and 100, 98 and 84% at 300°C, respectively.

Table 2. Flexural strength and modulus for test specimens.

Types	G1						G2		G3		C1	
Diameter	10 mm		16 mm		20 mm		10 mm		10 mm		10 mm	
Specimen	f_b (MPa)	E_b (GPa)	f_b (MPa)	E_b (GPa)	f_b (MPa)	E_b (GPa)	f_b (MPa)	E_b (GPa)	f_b (MPa)	E_b (GPa)	f_b (MPa)	E_b (GPa)
Room Temperature	1055	46.1	773	45.9	942	54.9	1131	37.7	814	34.1	830	80.0
100-1h-i	823	45.4	652	44.2	793	45.4	1080	37.3	732	33.6	700	79.8
200-1h-i	710	32.9	246	8.4	176	10.1	806	26.1	516	26.2	538	37.9
300-1h-i	512	29.6	242	8.6	108	10.0	689	26.0	326	20.2	441	26.6
100-1h-C	1005	45.0	735	46.0	865	51.8	-	-	-	-	-	-
200-1h-C	909	45.8	738	45.2	849	50.5	-	-	-	-	-	-
300-1h-C	933	46.0	724	44.8	918	45.9	-	-	-	-	-	-

G1 G2 G1 G1

(a) 10 mm diameter (b) 20 mm diameter

Figure 3. The general typical failure mode of FRP bars after testing.

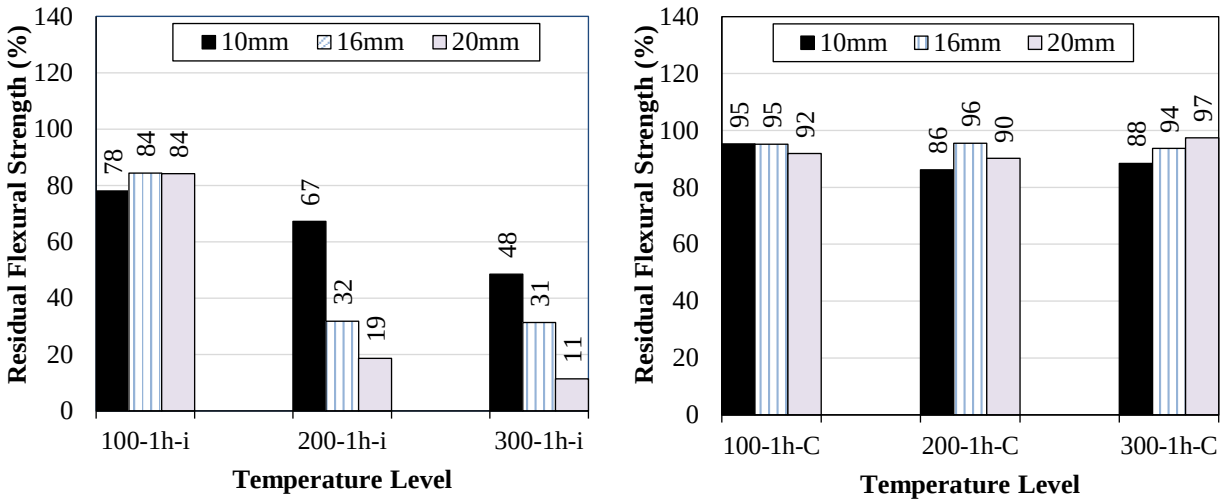

(a) (b)

Figure 4. Residual flexural strength of G1 at different temperatures: (a) immediate; (b) after cooling.

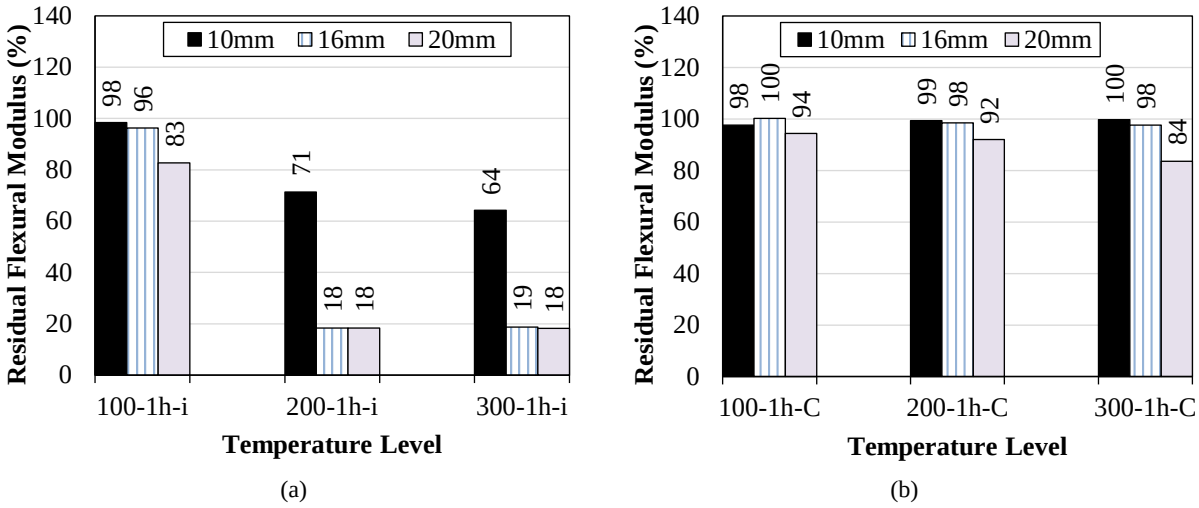

Figure 5. Residual flexural modulus of G1 at different temperatures: (a) immediate; and (b) after cooling.

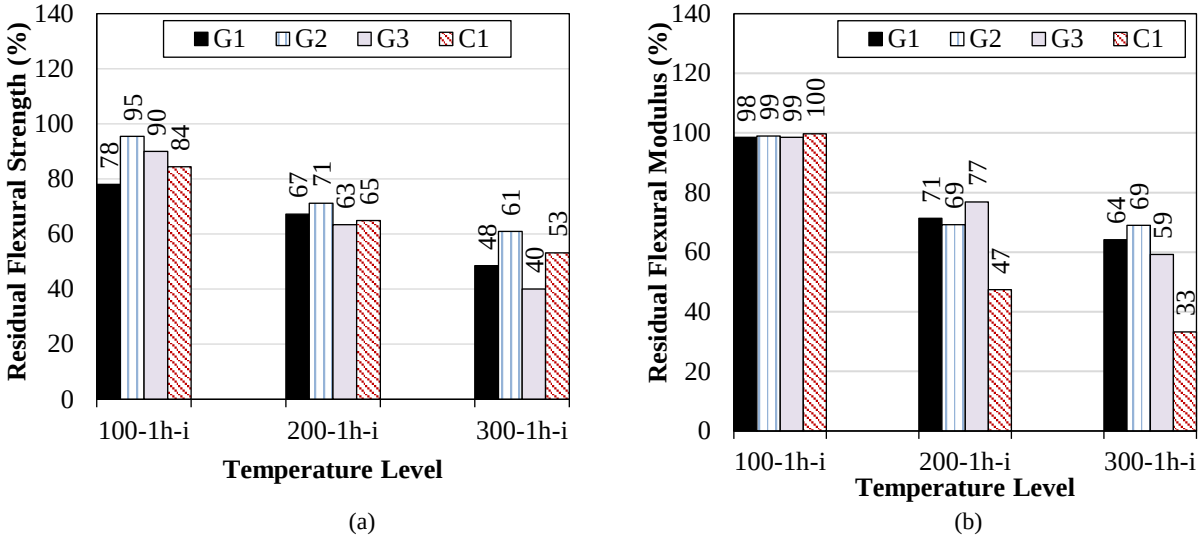

Figure 6. The behavior of different types of FRP bars exposed to different temperature levels: (a) residual flexural strength; (b) residual flexural modulus.

3.4. Effect of FRP Type

Figure (6a) shows the residual flexural strength of all types of FRP bars with a 10 mm diameter. Similar to type G1, the flexural strength of all FRP types decreased as the temperature level increased due to the resin decomposition at higher temperatures above the T_g (around 120°C). Therefore, a significant decrease of the flexural strength occurred because the polymer lost part of its ability to hold the fibre and to transfer the stresses between fibres. All types showed close residual flexure strengths at different temperatures. The residual flexure strength values ranged from 78 to 95%, 63 to 71, and 40 to 61% at 100, 200, and 300°C, respectively. However, at all temperature levels, type G2 (sand coated GFRP bars) showed the highest residual flexural strength compared to other types. The relationship between the flexural modulus and temperature is shown in Fig. 6(b). It can be seen that the flexural modulus was not affected at 100°C. For both 200 and 300°C, the flexural modulus was significantly decreased for all FRP types. The residual flexural modulus of the GFRP bars at 200 and 300°C ranged from 69 to 77% and 59 to 69, respectively. The CFRP bars (C1), however, showed the lowest residual flexural modulus among all types with losses of about 53 and 67% at 200 and 300°C, respectively. This may point to a weaker contact between the matrix and the carbon fibres at a temperature higher than the T_g. It may be also due to the type of matrix used in manufacturing the carbon bars. Additional studies are required in the future to clarify this point.

4. CONCLUSION

Based on the test results of this research, the following conclusions can be drawn:

- The flexural strengths and moduli of all immediately tested specimens decreased as the temperature level increased. For all 10mm diameter bars, the residual flexural strengths ranged between 40 and 61%, while the residual flexure moduli ranged between 33 and 69%, after exposure to 300℃.
- Bars with larger diameters showed lower residual flexural strengths and moduli compared to smaller diameter bars. The bars with 10, 16, and 20 mm diameters tested immediately after exposure to 300℃ showed residual flexural strengths of 48, 31, and 11%, respectively.
- At 200 and 300℃, the immediately tested G1 specimens showed significant flexural strength and moduli losses (29 to 89%) compared to the losses in the G1 bars tested after cooling to room temperature (0 to 16%).
- All tested GFRP bars showed comparable behavior at different temperatures. However, type G3 showed the highest flexural strength losses (37 and 60%) and type G2 bars showed the lowest losses (29 and 39%) after exposure to 200 and 300℃, respectively.
- The carbon FRP bars showed residual flexural strength ratios comparable to those of the GFRP bars; however, they showed lower residual flexural modulus ratios at 200 and 300℃.

CONFLICT OF INTEREST

The authors declare no conflict of interest.

FUNDING

This study was funded by the Department of Civil and Architectural Engineering, College of Engineering, Sultan Qaboos University, Oman.

ACKNOWLEDGMENT

The authors would like to acknowledge Sultan Qaboos University, the Civil and Architectural Engineering Department, and all the technicians at the structural laboratory for their help and support.

REFERENCES

Alsayed, S., Al-Salloum, Y., Almusallam, T., El-Gamal, S., Aqel, M. (2012). Performance of Glass Fiber Reinforced Polymer Bars under Elevated Temperatures. *Composites Part B*, Vol. 43, pp. 2265-2271.

Ashrafi, H., Bazli, M., Najafabadi, M., Oskouei, A. (2017). The Effect of Mechanical and Thermal Properties of FRP Bars on Their Tensile Performance under Elevated Temperatures. *Construction and Building Materials*, Vol. 157, pp. 1001–1010.

ASTM D790-03 (2003). Standard Test Methods for Flexural Properties of Unreinforced and Reinforced Plastics and Electrical Insulating Materials. *ASTM International*, West Conshohocken, PA, USA.

Bazli M, Abolfazli M (2020), Mechanical Properties of Fibre Reinforced Polymers under Elevated Temperatures: An Overview. *Polymers* 12, 2600; doi:10.3390/polym12112600.

Benmokrane, B., Eisa, M., El-Gamel, S., Denis, T., El-Salakawy, E. (2008). Pavement system suiting local conditions. *ACI Concrete International Magazine*. November 2008: pp.34-39.

Benmokrane, B., El-Salakawy, E., El-Ragaby, A., and El-Gamal, S.E. (2007). Performance evaluation of innovative concrete bridge deck slabs reinforced with fibre-reinforced-polymer bars. *Canadian Journal of Civil Engineering*, 34(3), 298-310.

Bouguerra, K., Ahmed E.A., El-Gamal, S.E., and Benmokrane, B. (2011). Testing of full-scale concrete bridge deck slabs reinforced with Fiber Reinforced Polymer (FRP) bars. *Construction and Building Materials Journal*, Vol. 25, 3956–3965.

Dulude, C., Ahmed, E., El-Gamal, S., Benmokrane, B. (2011). Testing of large-scale two-way concrete slabs reinforced with GFRP bars. *Advances in FRP Composites in Civil Engineering*, 287-291.

El-Gamal, S.E., Abdul Rahman, B., Benmokrane, B (2010). Deflection Behavior of Concrete Beams Reinforced with Different Types of GFRP Bars. The 5th International Conference on FRP Composites in Civil Engineering, Beijing, China, Sept. 27-29

El-Gamal, S.E., Al-Nuaimi, A., Al-Saidy, A., Al-Lawati, A. (2014). Flexural strengthening of RC beams using near-surface mounted fibre reinforced polymers. *The Brunei International Conference on Engineering and Technology*, Institut Teknologi Brunei, Brunei Darussalam, November 1-3, 10p.

El-Gamal, S.E., AlShareedah, O. (2020a). The behavior of axially loaded low strength concrete columns reinforced with GFRP bars and spirals. *Engineering Structures*, 216, 110732

El-Gamal, S.E., AlShareedah, O. (2020b). Experimental study on the performance of circular concrete columns reinforced with GFRP under axial load. *International Conference on Civil Infrastructure and Construction* (*CIC 2020*), February 2-5, 2020, Doha, Qatar.

El-Gamal, S.E., Benmokrane, B., and El-Salakawy, E.F. (2009). Cracking and deflection behavior of one-way parking garage slabs reinforced with CFRP bars. *ACI Special Publication*, SP-264-3, 33-52.

Hamad, R., Johari, M., Haddad, R. (2017). Mechanical properties and bond characteristics of different fiber reinforced polymer rebars at elevated temperatures. *Construction and Building Materials*, Vol. 142, pp. 521-535.

Hibbeler, R.C. (2018). Structural Analysis, *10th Edition in SI Units*, Pearson, Prentice Hall, pp. 700.

Jafarzadeh H, Nematzadeh M (2020), Evaluation of post-heating flexural behavior of steel fiber-reinforced high-strength concrete beams reinforced with FRP bars: Experimental and analytical results**.** *Engineering Structures* 225: 111292.

Maranan, G., Manalo, A., Karunasena, B., Benmokrane, B., Lutze, D. (2014). Flexural behavior of glass fibre reinforced polymer (GFRP) bars subjected to elevated temperature. *The 23rd Australasian Conference on the Mechanics of Structures and Materials* (*ACMSM23*), Vol. I, Byron Bay.

Robert, M., Benmokrane, B. (2010). Behavior of GFRP reinforcing bars subjected to extreme temperatures. *Journal of Composites for Construction*, Vol. 14, No. 1, pp. 353-360.

Thébeau, D., Benmokrane, B., and El-Gamal S.E. (2010). Three-year performance of continuously reinforced concrete pavement with GFRP bars. *The 11th International Symposium on Concrete Roads*, Seville, Spain, October 13-15, 11p.

Appendix A: Eqn. (1): Flexure Strength (fb)
The flexural strength was derived using the following equations (Hibbler R.C. 2018):

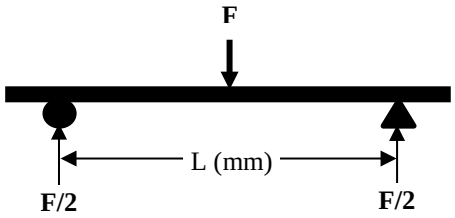

$$f_b = \frac{M}{I} y \quad \text{(A1)}$$

where f_b is the flexural strength of the FRP bar (N/mm2); M is maximum bending moment under the load (N.mm); I is the moment of inertia of the FRP bar about its neutral axis (mm4), y is the perpendicular distance from the neutral axis of the FRP bar to its outer surface (mm).

$$M = \frac{F}{2}\left(\frac{L}{2}\right) = \frac{FL}{4} \quad \text{(A2)}$$

$$y = \frac{d}{2} \quad \text{(A3)}$$

$$I = 0.25\,\pi\,(\frac{d}{2})^4 \quad \text{(A4)}$$

where, d is the diameter of the GFRP bar (mm)
Substituting Eqns. (A2), (A3) and (A4) into Eqn. (A1) results in:

$$f_b = \frac{FL}{4 \times 0.25\,\pi\left(\frac{d}{2}\right)^4}\,\frac{d}{2} \quad \text{(A5)}$$

$$f_b = \frac{8FL}{\pi\, d^3} \quad \text{(A6)}$$

Appendix B: Eqn. (2): Flexure Modulus, (Eb)
The calculations of the flexural modulus were derived using the double integration method given in (Hibbler R.C. 2018).

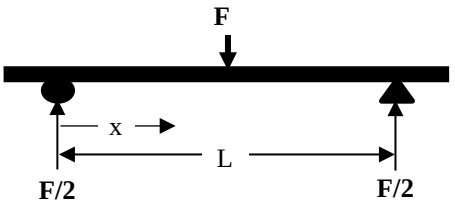

$$\frac{d^2v}{dx^2} = \frac{M}{EI} = \frac{Fx}{2EI} \quad \text{(B1)}$$

$$EI\,\frac{dv}{dx} = \int_0^x \frac{Fx}{2}\,dx = \frac{Fx^2}{4} + C1 \quad \text{(B2)}$$

$$EI\Delta = \int_0^x (\frac{Fx^2}{4} + C1)\,dx = \frac{Fx^3}{12} + C1x + C2 \quad \text{(B3)}$$

At $x = \frac{L}{2} \quad \rightarrow \quad \frac{dv}{dx} = 0$

From 1, $0 = \frac{F(\frac{L}{2})^2}{4} + C1 \rightarrow C1 = -\frac{FL^2}{16}$ (B4)

At $x = 0 \quad \rightarrow \quad \Delta = 0$

From 2, $0 = 0 + 0 + C2 \rightarrow C2 = 0$ (B5)

By substituting the values of C1 and C2 into Eqn. (B3),

$$EI\Delta = \frac{Fx^3}{12} - \frac{FL^2}{16}x \quad \text{(B6)}$$

At x = L/2, $\Delta = \Delta_{max}$

$$EI\Delta_{max} = \frac{F(\frac{L}{2})^3}{12} - \frac{FL^2}{12}\left(\frac{L}{2}\right) = \frac{-2FL^3}{96} \quad \text{(B7)}$$

$$E_b = \frac{-2FL^3}{96\,I\Delta_{max}} = \frac{-F}{\Delta_{max}}\,\frac{2L^3}{96\left(0.25\,\pi\left(\frac{d}{2}\right)^4\right)} \quad \text{(B8)}$$

$$E_b = \frac{-F}{\Delta}\,\frac{4L^3}{3\,\pi\, d^4} \quad \text{(B9)}$$